Enhanced Signal Sets for Hybrid Reflection Modulation

Nabarun Roy and Ananthanarayanan Chockalingam

***Abstract*—Hybrid reflection modulation (HRM) is a promising modulation technique which employs a combination of active and passive reflecting elements in reconfigurable intelligent surfaces (RIS). In addition to applying phase tuning, the active elements apply an amplification to its incident signal, which can alleviate the double-fading effect inherent in RIS systems. The choice of the elements to be made active conveys information bits through indexing. Additional bits can be conveyed through symbols from a modulation alphabet. In this paper, we propose methods to design improved HRM signal sets that achieve better bit error performance. The idea is to schedule the activation of tiles of elements in an ordered way that picks tiles with highest effective response and ignores those with lowest effective response. Specifically, we propose a signal set design procedure that efficiently packs non-equidistant signal points on the positive real line when all active elements use the same amplification factor. We further improve this signal set by obtaining the optimum amplification factors that maximize the minimum Euclidean distance of the signal set. Simulation results show improved performance of the proposed HRM signal sets compared to the that of basic HRM signal set introduced in the recent literature.**

***Index Terms*—Reconfigurable intelligent surface, hybrid reflection modulation, amplification optimization, constellation design.**

I. Introduction

Reconfigurable intelligent surfaces (RIS) have emerged as a key technology for enhancing signal quality, coverage, and energy efficiency in next-generation wireless networks [1],[2]. RIS are smart surfaces composed of an array of large number of programmable reflecting elements. By adjusting the phase of these elements, RIS can reflect incident electromagnetic waves to maximize their directivity towards the receiver, resulting in substantial signal-to-noise ratio (SNR) gains. The nearly passive nature of RIS requiring only static power for reconfiguring the elements is a key advantage. This leads to very low energy consumption and high energy efficiency [3]. Investigation in [4] shows that the RIS can effectively reduce transmit power and achieve a power scaling law proportional to N^2 (where N is the number of reflecting elements in the RIS). Moreover, it has been shown that significant performance improvements can be achieved through the deployment of RIS in various wireless systems, including orthogonal frequency division multiplexing (OFDM) [5], orthogonal time frequency space modulation (OTFS) [6], non-orthogonal multiple access (NOMA) [7], and Internet of Things (IoT) networks [8].

Despite the several advantages offered by RIS, there are inherent limitations associated with it. As reported in [2], RIS suffer from double or multiplicative fading effect. In RIS-aided systems, the overall channel response from transmitter to receiver can be obtained as the product of channel responses of the transmitter-RIS and RIS-receiver links. The resulting attenuation can be several orders of magnitude less than the direct channel from the transmitter to the receiver. To mitigate the attenuation effect, multiple relays are employed or large number of reflecting elements is deployed at the RIS. Research from [9] shows that to achieve comparable performance with the classical relay-aided system in practice, the passive RIS requires a prohibitively large number of elements. Use of active RIS elements, recently proposed in the literature, is an alternate approach to mitigate the attenuation. In contrast to conventional passive RIS that simply reflects the incoming signals, active RIS employs amplifiers to magnify them, which can effectively compensate the double fading loss. Investigations in [10] show significantly more gain in active RIS than in passive RIS when compared to system without RIS.

Index modulation (IM) is an important physical layer technique, where information bits are conveyed through indexing of transmission entities such as transmission antennas in multi-antenna systems, subcarriers in OFDM systems, and delay-Doppler bins for OTFS systems [11],[12]. The authors of [13] introduce a novel hybrid reflection modulation (HRM) scheme, which utilizes active RIS elements not only to mitigate double fading but also to encode information bits through IM. In HRM, all elements perform phase tuning while some selected elements perform signal amplification as well, and which elements are activated for amplification is determined by IM bits. Encoding information bits through IM of reflecting elements has been studied in reflective index modulation (RIM) [14] and reflective group number based index modulation (RGNIM) [15], where all reflecting elements are passive for phase tuning only and there are no active elements for amplification. On the other hand, HRM uses both passive and active elements along with IM. The findings in [13] show a substantial performance advantage of HRM over conventional passive RIS systems. Motivated by the HRM scheme, we build further on the basic HRM framework in [13], and delve deeper into optimization possibilities in the existing HRM scheme. Specifically, in this letter, we propose methods to design improved HRM signal sets that achieve better bit error performance. Specifically, we first propose a signal set design procedure that efficiently packs non-equidistant signal points on the positive real line when all active elements use the same amplification factor. Next, we further improve this signal set by obtaining optimum amplification factors that maximize the minimum Euclidean distance of the signal set. Simulation results show improved performance of the proposed HRM signal sets compared to the basic HRM signal set.

Manuscript submitted December 1, 2024; revised February 4, 2025; accepted February 7, 2025. This work was supported in part by the J. C. Bose National Fellowship, Department of Science and Technology, Government of India. The associate editor coordinating the review of this paper and approving it for publication was Dr. Petros S. Bithas. (*Corresponding author: A. Chockalingam.)*

The authors are with the Department of ECE, Indian Institute of Science, Bangalore, India, 560012. E-mail: {nabarunroy; achockal}@iisc.ac.in.

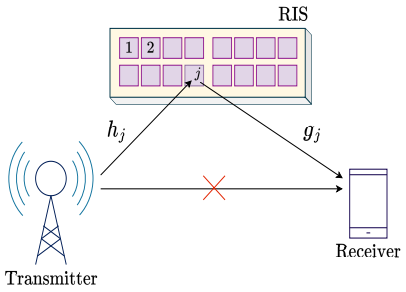

Fig. 1. HRM system model.

II. HRM SYSTEM MODEL

Here, we introduce the basic HRM scheme with single tone and complex modulation symbols [13]. Figure 1 shows an RIS-aided single-input single-output (SISO) system having N reflecting elements in the RIS. The channel coefficients from the transmitter to jth RIS element and from jth element to the receiver are denoted by h_j and g_j, respectively. The direct link between the transmitter and receiver is assumed to be blocked. Denoting the pathloss factors associated with the Tx-RIS and RIS-Rx links as L_t and L_r, respectively, the effective Tx-Rx channel response through the jth reflecting element is

$$\begin{aligned}\tilde{h}_j &= a_j\sqrt{L_t}h_j\sqrt{L_r}g_j\exp\{\mathrm{j}\phi_j\} \\ &= a_j\sqrt{L_tL_r}|h_j||g_j|\exp\{\mathrm{j}(\angle h_j+\angle g_j+\phi_j)\}, \quad (1)\end{aligned}$$

where $\mathrm{j}=\sqrt{-1}$, a_j is the amplification factor ($a_j=1$ for passive element, $a_j>1$ for active element) and ϕ_j is the tunable phase associated with jth element. The objective is to optimize the phase shifts to maximize the overall channel response towards the receiver. Considering optimum phase shift for the jth element, i.e., $\phi_{j,\text{opt}}=-(\angle h_j+\angle g_j)$, the effective channel response, $\tilde{h}_{j,\text{opt}}$ is given by $\tilde{h}_{j,\text{opt}}=a_j\sqrt{L_tL_r}|h_j||g_j|$.

A. HRM with single tone and complex modulation symbols

HRM can be realized with a single tone (Fig. 2a) or with complex modulation symbols (Fig. 2b). In HRM with single tone, bits are conveyed only through indexing of reflecting elements in the RIS. In HRM with complex modulation symbols, additional information bits are conveyed through complex modulation symbols, e.g., QAM/QPK symbols.

In HRM with single tone, the RIS having N reflecting elements is partitioned into G tiles, where each tile consists of S reflecting elements, i.e., $S=\frac{N}{G}$. The elements are activated tile-wise. That is, a tile is said to be active if all its elements are active (i.e., each element of the active tile performs power amplification in addition to phase tuning). In tiles which are not active (i.e., passive), all the elements in them perform only phase tuning. The number of tiles to be activated is decided by information bits, i.e., each bit sequence corresponds to unique number of active tiles. Figure 3 shows an example of active/passive tiles arrangement in a HRM system with an RIS that has 32 reflecting elements ($N=32$), which are symmetrically partitioned into 4 tiles ($G=4$), with 8 elements ($S=8$) in each tile. Red elements are active and blue elements are passive. Figures 3(a), (b), (c), and (d) show the active/passive tile arrangement corresponding to information bit sequences {0 0}, {0 1}, {1 0}, and {1 1}, respectively, where 0, 1, 2, and 3 tiles, respectively, are activated.

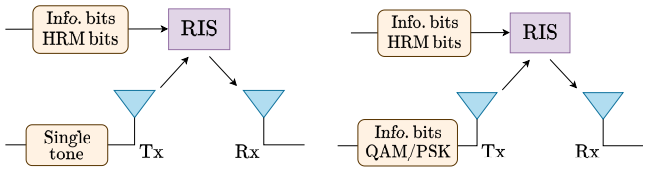

(a) With single tone (b) With complex modulation symbols

Fig. 2. HRM scheme.

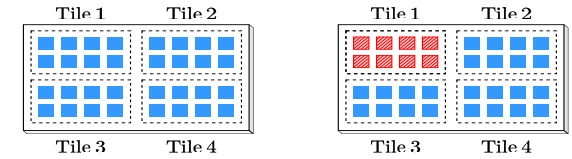

(a) HRM, w_1, bit seq. = {0 0} (b) HRM, w_2, bit seq. = {0 1}

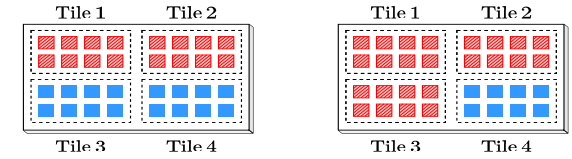

(c) HRM, w_3, bit seq. = {1 0} (d) HRM, w_4, bit seq. = {1 1}

Fig. 3. An example active/passive tiles arrangement and corresponding bit sequences in HRM with $N=32$, $G=4$, $S=8$. Red elements: active. Blue elements: passive.

Construction of HRM signal set: Let s_i denote the effective channel response for the ith tile in the RIS. Assuming phase optimized RIS elements, s_i can be computed as

$$s_i=\sqrt{L_tL_r}\sum_{j=(i-1)S+1}^{iS}|h_j||g_j|, \quad i=1,\cdots,G. \quad (2)$$

Since there is no direct path, the overall channel response of a HRM system, w, having G tiles can be expressed as

$$w=\sum_{i=1}^{G}a_is_i, \quad (3)$$

where a_i is the amplification gain for the ith tile with $a_i=1$ if the tile is passive and $a_i>1$ if the tile is active. In the basic HRM scheme, uniform amplification factor is applied across all the active tiles, i.e., $a_i=a$, $\forall i$. Consequently, the channel alphabet $\mathbb{W}_{\text{hrm}}=\{w_1,w_2,\cdots,w_G\}$, where w_n, $n=1,2,\cdots,G$, is expressed as

$$w_n=\sum_{i=1}^{G}s_i+\sum_{j=1}^{n-1}(a-1)s_j, \quad (4)$$

where a is the constant amplification factor associated with each tile in the RIS. The achieved rate in HRM with single tone, in bits per channel use (bpcu), is given by $\lfloor\log_2 G\rfloor$. Note that the tile activation schedule (i.e., mapping information bit sequence to tiles activation) is such that, in the example in Fig. 3, no tiles are activated for bit sequence 00; tile 1 is activated for bit sequence 01; tiles 1 and 2 are activated for bit sequence 10; and tiles 1, 2, and 3 are activated for bit sequence 11. The received signal at the receiver can be written as

$$y=\sqrt{P_t}w+n, \quad (5)$$

where $w\in\mathbb{W}_{\text{hrm}}$, P_t is the transmit power, and n is the noise. Likewise, in HRM with complex modulation symbols, the received signal can be written as

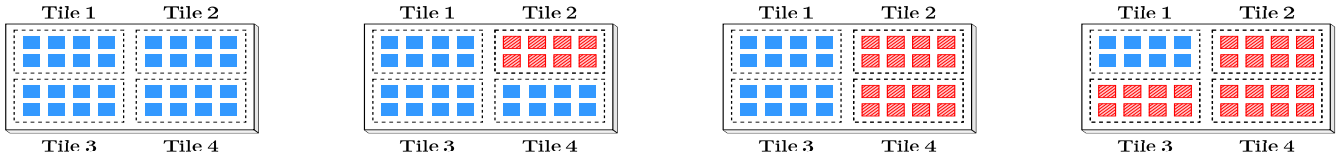

(a) HRM-E1, w'_1, bit seq. = {0 0} (b) HRM-E1, w'_2, bit seq. = {0 1} (c) HRM-E1, w'_3, bit seq. = {1 0} (d) HRM-E1, w'_4, bit seq. = {1 1}

Fig. 4. Active/passive tiles arrangement and corresponding bit sequences in HRM-E1 with $N = 32$, $G = 4$, $S = 8$, $s_2 > s_4 > s_3 > s_1$ (i.e., $s'_1 = s_2,\ s'_2 = s_4,\ s'_3 = s_3,\ s'_4 = s_1$). Red elements: active. Blue elements: passive.

$$y = \sqrt{P_t} w x + n, \tag{6}$$

where $w \in \mathbb{W}_{\text{hrm}}$ and $x \in \mathbb{A}$, where $\mathbb{A}$ is the complex modulation alphabet. The achieved rate in HRM with complex symbol modulation is $\lfloor \log_2 G \rfloor + \lfloor \log_2 |\mathbb{A}| \rfloor$ bpcu.

III. Enhanced signal sets for HRM

In this section, we propose new signal sets for HRM which aim to enhance the performance of the basic HRM presented in the previous section. We call the proposed signal sets as HRM-E1 and HRM-E2 signal sets. HRM-E1 signal set is devised based on improved tile scheduling and HRM-E2 signal set is based on optimizing the amplification factors of the tiles.

A. HRM-E1 signal set

The HRM-E1 scheme, like the basic HRM scheme, uses same amplification factor for all the tiles. However, the tile scheduling (information bit sequence to active tiles mapping) is different. The tile scheduling is improved by having tiles ordered on the basis of the magnitude of their effective channel coefficients. The HRM-E1 signal set is constructed as follows.

Let $\mathbb{S} = \{s_1, s_2, \cdots, s_G\}$ be the set consisting of the effective channel response of all the tiles of the RIS (see Eq. (2)) and let $\mathbb{S}' = \{s'_1, s'_2, \cdots, s'_G\}$ be derived by arranging the elements of $\mathbb{S}$ in descending order. That is, $s'_1 = \max\{s_1, s_2, \cdots, s_G\}$, $s'_2 = \max\{\{s_1, s_2, \cdots, s_G\} \backslash s'_1\}$ so that, in general, $s'_k = \max\{\{s_1, s_2, \cdots, s_G\} \backslash \{s'_1, s'_2, \cdots, s'_{k-1}\}\}$. The HRM-E1 signal set, $\mathbb{W}_{\text{hrm-E1}} = \{w'_1, w'_2, \cdots, w'_G\}$, is obtained as

$$w'_n = \sum_{i=1}^{G} s'_i + \sum_{j=1}^{n-1} (a-1) s'_j, \qquad n = 1, 2, \cdots, G. \tag{7}$$

where a is the common amplification factor associated with each tile. Now, the tile scheduling is similar to that in the basic HRM except that the unordered $\{s_i\}$s are replaced with ordered $\{s'_i\}$s. By ordering the tiles, it is ensured that for every signal point, the tile with the highest effective response is activated among the other available tiles. Furthermore, by scheduling tiles in descending order, the tile with the lowest effective response is never activated. This approach enhances the minimum Euclidean distance between the signal points in the signal set, thereby improving BER performance. For scheduling tiles, existing low-complexity sorting algorithms can be utilized. For instance, merge sort can be used which has complexity of order $\mathcal{O}(G \log(G))$ [16]. Figure 4 shows the tile scheduling in HRM-E1 corresponding to the HRM tile scheduling example in Fig. 3 where the effective channel magnitudes are such that $s_2 > s_4 > s_3 > s_1$ (i.e., $s'_1 = s_2,\ s'_2 = s_4,\ s'_3 = s_3,\ s'_4 = s_1$). Note that, in this HRM-E1 tile scheduling example, no tiles are activated for bit sequence 00; tile 2 is activated for bit sequence 01; tiles 2 and 4 are activated for bit sequence 10; and tiles 2, 3, and 4 are activated for bit sequence 11. Note that the tile activation schedules for HRM-E1 (Fig. 4) and HRM (Fig. 3) are different. The received signal in HRM-E1 scheme with complex modulation symbols is given by

$$y = \sqrt{P_t} w' x + n = \sqrt{P_t} u' + n, \tag{8}$$

where $w' \in \mathbb{W}_{\text{hrm-E1}}$, $x \in \mathbb{A}$, and $u' \in \mathbb{U}$, defined as $\mathbb{U} = \{u'^q_p : u'^q_p = w'_p x_q,\ \forall\ p \in \{1, 2, \cdots G\}, q \in \{1, 2, \cdots |\mathbb{A}|\}\}$. Substituting $x = 1$ in (8) will give the received signal in HRM-E1 scheme with single tone.

B. HRM-E2 signal set

HRM-E2 scheme differs from the basic HRM scheme on two counts; one, the tile activation schedule is different, and, two, the amplification factors are different for different tiles. The tile activation schedule in HRM-E2 is the same as that of HRM-E1. The amplification factors for different tiles in HRM-E2 are optimized as follows.

Let $\mathbb{S}' = \{s'_1, \cdots, s'_G\}$ denote the set of effective channel responses of the tiles in descending order of their magnitudes and let $\{a_1, \cdots, a_G\}$ denote their corresponding amplification factors, i.e., a_i is the amplification factor of the ith tile. The HRM-E2 signal set, $\mathbb{W}_{\text{hrm-E2}} = \{\bar{w}_1, \cdots, \bar{w}_G\}$, is given by

$$\bar{w}_n = \sum_{i=1}^{G} s'_i + \sum_{j=1}^{n-1} (a_j - 1) s'_j, \qquad n = 1, 2, \cdots, G, \tag{9}$$

and the received signal is given by $y = \sqrt{P_t} \bar{w} + n$, where $\bar{w} \in \mathbb{W}_{\text{hrm-E2}}$.

Optimized amplification factor for each tile: To obtain the optimized amplification factor for each tile, we maximize the minimum distance of the signal set with same total average active power constraint, P_a. In the case of HRM and HRM-E1 with constant amplification factor a for all the tiles, $P_a = \tilde{N}_{\text{a}} a^2$, where $\tilde{N}_{\text{a}}$ is the total number of active elements averaged over all possible information bit sequences, which, for an RIS with N elements and G tiles can be computed as

$$\tilde{N}_{\text{a}} = \frac{N}{G^2} \sum_{k=1}^{G-1} k. \tag{10}$$

In the case of HRM-E2 with amplification factor a_i for the ith tile, the total average active power is given by

$$P_a = \frac{S}{G} \sum_{k=1}^{G-1} (G-k) a_k^2. \tag{11}$$

The Gth tile remains inactive for all possible transmission bit sequences, as shown in Fig. 3 for the HRM scheme

(where tile 4 is inactive for all transmission bit sequences) and Fig. 4 for HRM-E1 and HRM-E2 schemes (where tile 1 is inactive across all bit sequences). As the Gth tile does not contribute to the signal amplification process, its associated amplification gain is not considered for the computation of the total average active power. Consequently, the optimization problem to determine the $G-1$ optimal amplification factors for the tiles actively involved in signal amplification, aimed at maximizing the minimum distance of the signal set, can be formulated as follows:

$$\{\hat{a}_1, \hat{a}_2, \cdots, \hat{a}_{G-1}\} = \underset{\{a_1,a_2,\cdots,a_{G-1}\}}{\text{argmax}} \min |\bar{w}_j - \bar{w}_i| \quad (12)$$
$$\forall\, i \neq j; i, j \in \{1, 2, \cdots G\},$$
$$\text{s.t.} \quad \frac{N}{G^2}\sum_{k=1}^{G-1}(G-k)a_k^2 = P_{\text{a}} = \frac{N(G-1)a^2}{2G}, \quad (13)$$

Without loss of generality, we can consider $j > i$ as objective function is modulus of the difference, which will be positive. Now, $|\bar{w}_j - \bar{w}_i|$ can be expressed as

$$|\bar{w}_j - \bar{w}_i| = \sum_{k=i}^{j-1}(a_k - 1)s'_k. \quad (14)$$

As s'_ks are positive quantities and amplification factors $a_k > 1$, $|\bar{w}_i - \bar{w}_j|$ will achieve the minimum value when $|j-i| = 1$. Hence, the optimization problem can be reframed as

$$\{\hat{a}_1, \hat{a}_2, \cdots, \hat{a}_{G-1}\} = \underset{\{a_1,a_2,\cdots,a_{G-1}\}}{\text{argmax}} \min |\bar{w}_{i+1} - \bar{w}_i|$$
$$= \underset{\{a_1,a_2,\cdots,a_{G-1}\}}{\text{argmax}} \min(a_i - 1)s'_i,\ \forall\, i \in \{1, 2, \cdots G-1\}, \quad (15)$$

with the power constraint in (13).

The global optimal solution approach is to design the signal set (i.e., choosing the amplification factors) such that there is equal spacing between any two consecutive signal points in the signal set, which has the advantage of decoding simplicity. Towards this approach, let the distance between any two consecutive points in the signal set be t. That is, the minimization metric $|\bar{w}_{i+1} - \bar{w}_i| = (a_i - 1)s'_i$ in (15) is the same $(= t)$, $\forall i$. Accordingly, the amplification factors in terms of t can be expressed as

$$a_i = \frac{t}{s'_i} + 1, \quad i \in \{1, 2, \cdots, G-1\}. \quad (16)$$

Substituting a_is from (16) in the constraint in (13), we get

$$t^2 \sum_{k=1}^{G-1}\frac{G-k}{s'^2_k} + 2t\sum_{k=1}^{G-1}\frac{G-k}{s'_k} + \frac{G(G-1)}{2}(1-a^2) = 0. \quad (17)$$

Solving for t in (17) gives t as

$$\frac{-\sum_{k=1}^{G-1}\frac{G-k}{s'_k} + \sqrt{(\sum_{k=1}^{G-1}\frac{G-k}{s'_k})^2 + (\frac{G(G-1)}{2}(a^2-1))(\sum_{k=1}^{G-1}\frac{G-k}{s'^2_k})}}{\sum_{k=1}^{G-1}\frac{G-k}{s'^2_k}},$$

which when used in (16) gives the optimized amplification factors in closed-form. Using these optimized amplification factors in (9) gives the HRM-E2 signal set, $\mathbb{W}_{\text{hrm}-\text{E2}}$. Finding optimum a_is using (16) and t involves a complexity of order $\mathcal{O}(G)$. Table I summarizes the bit sequences and the corresponding number of active tiles, active tiles, and amplification factors corresponding to the example in Figs. 3 and 4. The received symbol for HRM-E2 scheme with complex modulation symbols is given by

$$y = \sqrt{P_t}\bar{w}x + n = \sqrt{P_t}\bar{u} + n, \quad (18)$$

where $\bar{w} \in \mathbb{W}_{\text{hrm}-\text{E2}}$, $x \in \mathbb{A}$, and $\bar{u} \in \mathbb{U}'$, defined as $\mathbb{U}' = \{\bar{u}^q_p : \bar{u}^q_p = \bar{w}_p x_q,\ \forall\, p \in \{1, 2, \cdots G\}, q \in \{1, 2, \cdots |\mathbb{A}|\}\}$.

TABLE I
BIT SEQUENCES AND CORRESPONDING NUMBER OF ACTIVE TILES (N_a), ACTIVE TILES, AND AMPLIFICATION FACTORS FOR VARIOUS HRM SCHEMES FOR THE EXAMPLES IN FIGS. 3 AND 4 WITH $s_2 > s_4 > s_3 > s_1$.

bit seq.	HRM			HRM-E1			HRM-E2		
	N_{a}	Active tiles	Amp. factors	N_{a}	Active tiles	Amp. factors	N_{a}	Active tiles	Amp. factors
{00}	0	-	-	0	-	-	0	-	-
{01}	1	1	a	1	2	a	1	2	a_1
{10}	2	1, 2	a, a	2	2, 4	a, a	2	2, 4	a_1, a_2
{11}	3	1, 2, 3	a, a, a	3	2, 4, 3	a, a, a	3	2, 4, 3	a_1, a_2, a_3

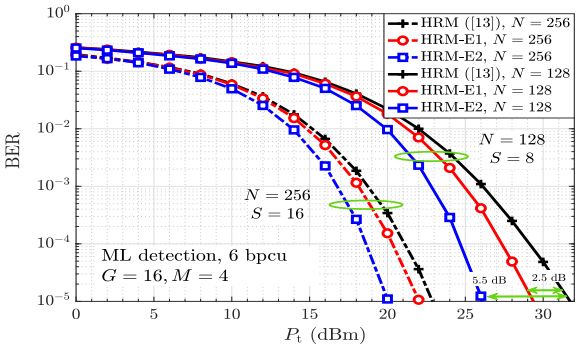

Fig. 5. BER performance of HRM, HRM-E1, and HRM-E2 schemes for different values of N at 6 bpcu rate.

IV. Results and Discussions

In this section, we present the simulated bit error rate (BER) performance of the HRM schemes and compare their relative performance. Analytical expressions for the BER can be obtained as in [13]. The simulation parameters are set as follows: the distance between the transmitter and RIS is assumed to be 20 meters, while the distance from the RIS to the receiver is taken as 50 meters. The corresponding path loss exponents are set to 2.2 for the transmitter-RIS link and 2.8 for the RIS-receiver link. In HRM schemes, in addition to static additive white Gaussian noise (AWGN), dynamic noise is introduced due to the activation of the reflecting elements at the RIS, as described in [13]. For the purpose of simulation, the noise variance for both static and dynamic noise components is set to -90 dBm. Additionally, a path loss value of -30 dB is considered at a reference distance of 1m.

Figure 5 presents a comparison of the BER performance of the basic HRM scheme in [13] with the performance of the proposed HRM-E1 and HRM-E2 schemes for different number of reflecting elements at the RIS ($N = 128, 256$) with $G = 16$, QPSK modulation ($M = 4$), and 6 bpcu rate. For HRM and HRM-E1, the constant amplification factor is set to $a = 10$. Maximum likelihood (ML) detection is used at the receiver. From Fig. 5, it can be observed that the HRM-E2 scheme outperforms HRM-E1, which, in turn, shows better performance compared to the HRM scheme. For example, for $N = 128$ and $S = 8$, at a BER of 10^{-5}, the proposed HRM-E1 performs better than HRM by about

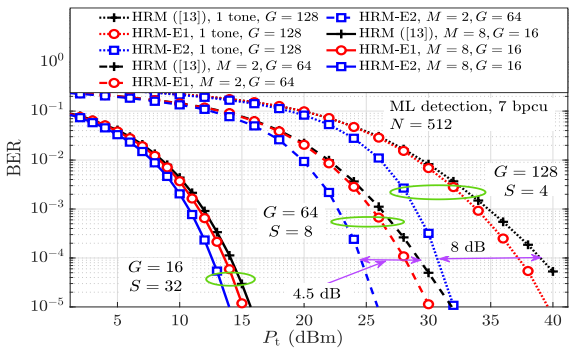

Fig. 6. BER performance of HRM, HRM-E1, and HRM-E2 schemes for different values of M and G for a given N and 7 bpcu rate.

2.5 dB. Also, HRM-E2 performs better than HRM by about 5.5 dB, demonstrating the performance improvement offered by the proposed amplification optimization. The performance improvement is more pronounced for smaller values of S. In other words, the performance gain is more for configurations with a smaller number of reflecting elements per tile.

Figure 6 shows a comparative BER performance of HRM, HRM-E1, and HRM-E2 schemes under different system configurations with the same number of reflecting elements at the RIS ($N = 512$). For the same N, the values of S, G, and M are chosen to achieve the same rate of 7 bpcu. For both HRM and HRM-E1, the constant amplification factor is set to $a = 10$. ML detection is used. From Fig. 6, it is seen that the proposed HRM-E1 and HRM-E2 schemes consistently outperform the HRM scheme for different system configurations with different constellation sizes $M = 2$ and 4 (i.e., BPSK and QPSK) including single-tone signaling ($M = 1$). For example, for single-tone signaling with $M = 1$ ($N = 512$, $G = 128$, $S = 4$), HRM-E2 gives a performance gain of about 8 dB compared to HRM at 10^{-4} BER, and the performance gain is about 4.5 dB for $M = 2$. Also, the performance with $M = 8$ is better than that with $M = 2$. Although an increase in M is expected to degrade performance, the corresponding decrease in G (to keep the rate same) enhances the effective tile response, which leads to better overall performance.

Figure 7 presents the BER performance of HRM, HRM-E1, and HRM-E2 schemes along with that of the RGNIM scheme in [15]. 8-QAM with Gray coding is used. The values of N and G are taken as 32 and 4, respectively. The constant amplification factor is set to $a = 1.85$. It is observed that the proposed HRM-E1 and HRM-E2 schemes achieve better BER performance compared to those of basic HRM and RGNIM schemes with perfect CSI. The figure also presents the comparative BER performances with imperfect CSI. As in [15], the channel between the RIS and the transmitter is assumed to be perfectly known, while the knowledge of the channel between the RIS and the receiver is imperfect, modeled as $\hat{g}_j = \rho g_j + \sqrt{(1-\rho^2)}\Delta g$, where ρ is the channel estimation accuracy parameter and Δg is Gaussian distributed $\mathcal{CN}(0,1)$ and independent of g_j [15]. With imperfect CSI, the proposed HRM-E2 scheme performs better than other schemes. For example, at 10^{-4} BER, HRM-E2 performs better than RGNIM by about 2 dB and 2.5 dB for perfect CSI and imperfect CSI (with $\rho = 0.99$), respectively.

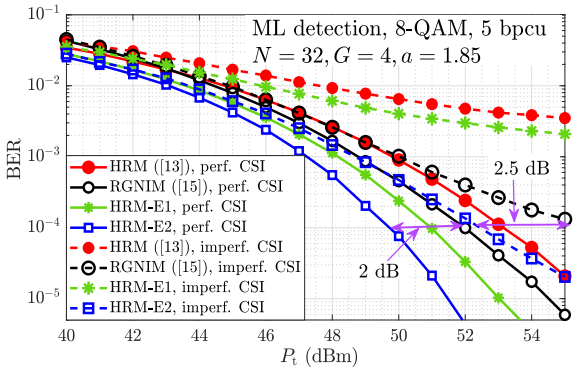

Fig. 7. BER performance of HRM, RGNIM, HRM-E1, and HRM-E2 schemes for 5 bpcu rate with perfect and imperfect CSI.

V. Conclusions

We proposed two enhanced signal sets for HRM, referred to as HRM-E1 and HRM-E2 signal sets. The enhanced signal sets are obtained through improved tile scheduling and optimization of the amplification factors. Our simulation results showed significant performance gains, ranging from 2 dB to 8 dB, in favor of the proposed signal sets compared to the basic HRM signal set. The improved performance can be attributed to the superior distance properties of the proposed signal sets. Future research directions include extension of the current study to multi-antenna systems in multiuser settings.

References

[1] E. Basar, M. D. Renzo, J. de Rosny, M. Debbah, M.-S. Alouini, and R. Zhang, "Wireless communications through reconfigurable intelligent surfaces," *IEEE Access*, vol. 7, pp. 116753-116773, Aug. 2019.

[2] Q. Wu, S. Zhang, B. Zheng, C. You, and R. Zhang, "Intelligent reflecting surface-aided wireless communications: A tutorial," *IEEE Trans. Commun.*, vol. 69, no. 5, pp. 3313–3351, May 2021.

[3] C. Huang, et al., "Reconfigurable intelligent surfaces for energy efficiency in wireless communication," *IEEE Trans. Wireless Commun.*, vol. 18, no. 8, pp. 4157-4170, Aug. 2019.

[4] Q. Wu and R. Zhang, "Intelligent reflecting surface enhanced wireless network via joint active and passive beamforming," *IEEE Trans. Wireless Commun.*, vol. 18, no. 11, pp. 5394-5409, Nov. 2019.

[5] Y. Yang, B. Zheng, S. Zhang, and R. Zhang, "Intelligent reflecting surface meets OFDM: protocol design and rate maximization," *IEEE Trans. Commun.*, vol. 68, no. 7, pp. 4522-4535, Jul. 2020.

[6] G. Harshavardhan, V. S. Bhat, A. Chockalingam, "RIS-aided OTFS modulation in high-Doppler channels," *IEEE PIMRC'2022*, Sep. 2022.

[7] J. Zhu et al., "Power efficient IRS-assisted NOMA," *IEEE Trans. Commun.*, vol. 69, no. 2, pp. 900-913, Feb. 2021.

[8] Z. Chu et al., "Intelligent reflecting surface assisted wireless powered sensor networks for Internet of Things," *IEEE Trans. Commun.*, vol. 69, no. 7, pp. 4877-4899, Jul. 2021.

[9] E. Björnson, Ö. Özdogan, and E. G. Larsson, "Intelligent reflecting surface versus decode-and-forward: how large surfaces are needed to beat relaying?," *IEEE Wireless Commun. Lett.*, vol. 9, pp. 244-248, Feb. 2020.

[10] Z. Zhang et al., "Active RIS vs. passive RIS: Which will prevail in 6G?," *IEEE Trans. Commun.*, vol. 71, no. 3, pp. 1707-1725, Mar. 2023.

[11] T. Mao et al., "Novel index modulation techniques: a survey," *IEEE Commun. Surveys & Tuts.*, vol. 21, no. 1, pp. 315-348, 2019.

[12] Y. I. Tek and E. Basar, "Joint delay-Doppler index modulation for orthogonal time frequency space modulation," *IEEE Trans. Commun.*, vol. 72, no. 7, pp. 3985-3993, Jul. 2024.

[13] Z. Yigit, E. Basar, M. Wen, I. Altunbas, "Hybrid reflection modulation," *IEEE Trans. Wireless Commun.*, vol. 22, no. 6, pp. 4106-4116, Jun. 2023.

[14] Y. Zhao, L. Zhang, J. Hu and K. Yang, "Reflective index modulation for IRS assisted integrated data and energy transfer," *IEEE Trans. Wireless Commun.*, vol. 23, no. 9, pp. 11508-11520, Sep. 2024.

[15] Y. Zhao et al., "Reflective group number based index modulation for intelligent reflecting surface assisted wireless communications," *Proc. IEEE ICC'2023*, pp. 265-270, May-Jun. 2023.

[16] R. Sedgewick and K. Wayne, *Algorithms,* Addison-Wesley, 2011.